PROCEEDINGS OF SCIENCE

Phenomenology of Spin-1 resonances at the LHC

Werner Porod*

University of Würzburg, Institute of Theoretical Physics and Astrophysics
Campus Hubland Nord, Emil-Hilb-Weg 22, D-97074 Würzburg, Germany

E-mail: werner.porod@uni-wuerzburg.de

Spin-1 resonances are among the states predicted by composite Higgs models and one expects them the have masses in the range of a few TeV. We focus here on models based on an underlying gauge-fermion description which predict QCD-coloured vector and axial-vector states as well as states charged under the electroweak gauge groups. The former can come as triplet, sextet and octet representation depending on the model details. All models considered have a colour octet vector state in common which can be singly produced at hadron colliders as it mixes with the gluon. We summarize here their LHC phenomenology and comment also on aspects relevant for future colliders.

Proceedings of the Corfu Summer Institute 2024 "School and Workshops on Elementary Particle Physics and Gravity" (CORFU2024) 12 - 26 May, and 25 August - 27 September, 2024
Corfu, Greece

*Speaker

 ISSN 1824-8039 . Published by SISSA Medialab.

1. Introduction

Composite Higgs models [1, 2] postulate the existence of an additional gauge interaction which becomes strong in the multi-TeV range. In this way, these models provide a potential solution to the problem of hierarchy between the electroweak scale and the Planck scale: like in quantum chromodynamics (QCD), the breaking scale is dynamically generated via confinement and condensation of the new interaction. The Higgs boson emerges as a pseudo Nambu Goldstone boson (pNGBs) [3] from the spontaneous breaking of the global symmetry in the new strong sector. Its potential is generated by explicit breaking terms: the gauging of the electroweak symmetry, the couplings of the top quark [4] and (eventually) a mass term for the underlying fermions [5, 6].

The largeness of the top-mass can be explained via partial compositeness [7] which leads to the prediction of top-partners. The fact, that these need to carry QCD charges implies that there are also coloured spin-0 and spin-1 states, as well as fermions carrying unusual colour charges. In this contribution, we focus on models based on an underlying gauge-fermion description as they allow for a systematic classification of the properties of the resonances. A systematic list of models describing the minimal resonances required by the Higgs sector has been presented in ref. [8]. An important class are model models with two separate species in different irreducible representations (irreps). A set of twelve minimal models, dubbed M1-M12, has been defined in ref. [9, 10] which are fully characterized in terms of the confining gauge group and the irreps and multiplicities of the two fermion species.

Several studies have been presented in the literature covering the phenomenology of various resonances of these twelve models: electroweak pNGBs [9, 11–13], singlets stemming from the global U(1)'s [9, 10, 14, 15], QCD coloured pNGBs [10, 16, 17], top partners with non-standard decays [18–22] or colour assignment [23], and spin-1 resonances carrying electroweak charges [24, 25] or QCD charges [26]. We note for completeness, that spectra and couplings of such resonances have been computed on the Lattice for models based on Sp(4) [27–33], e.g. models M5 and M8, and models based on SU(4) [34–39], e.g. models M6 and M11. Computations based on holography are also available [40–45]. The subset of models covered by both approaches give consistent results.

In this contribution we focus on the phenomenology of color charged spin-1 resonances which are present in all the models proposed in ref. [9, 10]. We summarize first relevant model aspects in the next section. We then discuss in the subsequent section to which extent this sector is constrained by existing LHC data. The final section concludes with a discussion and an outlook.

2. Model aspects

The models presented ef. [9, 10] propose that the hyperfermions charged under the new gauge come in two different representations such that top partners emerge as so called "chimera" baryons. These can be realized in two different patterns: $\psi\psi\chi$ and $\psi\chi\chi$, where ψ only carry electroweak charges while χ carry QCD colour and hypercharge. In the former case, the χ's QCD triplet carries hypercharge $2/3$, in the latter case $-1/3$. The spin-1 resonances carrying QCD charges emerge as bound states of the χ species. Their properties emerge from three types of cosets, SU(6)/SO(6), SU(6)/Sp(6) and SU(3)×SU(3)/SU(3).

	Models	$\chi\,(R,Y,B)$	π	$\mathcal{V}^\mu$	$\mathcal{A}^\mu$	Ψ	di-quark
C1	M1-2	$(\mathrm{R},-\frac{1}{3},\frac{1}{6})$	$8_0,\ 6_{-2/3}$	$8_0,\ 1_0,\ 3_{2/3}$	$8_0,\ 6_{-2/3}$	$8,\ 1,\ 3,\ 6$	none
C2	M3-4, M8-11	$(\mathrm{R},\frac{2}{3},\frac{1}{3})$	$8_0,\ 6_{4/3}$	$8_0,\ 1_0,\ 3_{-4/3}$	$8_0,\ 6_{4/3}$	3	$\pi_6, \mathcal{V}_3^\mu, \mathcal{A}_6^\mu$
C3	M5	$(\mathrm{Pr},-\frac{1}{3},\frac{1}{6})$	$8_0,\ 3_{2/3}$	$8_0,\ 1_0,\ 6_{-2/3}$	$8_0,\ 3_{2/3}$	$8,\ 1,\ 3,\ 6$	none
C4	M6-7	$(\mathrm{C},-\frac{1}{3},\frac{1}{6})$	8_0	$8_0,\ 1_0$	8_0	$8,\ 1,\ 3,\ 6$	none
C5	M12	$(\mathrm{C},\frac{2}{3},\frac{1}{3})$	8_0	$8_0,\ 1_0$	8_0	3	none

Table 1: Properties of the spin-0 (π), spin-1 ($\mathcal{V}^\mu$, $\mathcal{A}^\mu$) and spin-1/2 (Ψ) lightest resonances in the 12 models, grouped in 5 classes. Each class is determined by the properties of the χ species, listed in the second column by irrep type: R for real, Pr for pseudo-real and C for complex. For the resonances, the colours indicate the baryon numbers: black for $B = 0$, red for $B = \pm 1/3$ and blue for $B = \pm 2/3$. In the last column we indicate the bosons that can decay into a tt di-quark state.

The resulting spectrum contains a set of vectors $\mathcal{V}^\mu$ as well as a set of axial-vectors $\mathcal{A}^\mu$, which decay respectively into two or three pNGBs[1]. The latter property originates from the symmetric nature of the cosets [26]. All cosets contain an ubiquitous octet $\mathcal{V}_8^\mu$ within $\mathcal{V}^\mu$ which mixes with the QCD gluons. In addition there is always a color singlet within $\mathcal{V}^\mu$, a color octet within $\mathcal{A}^\mu$ as well as a color octet pNGB π_8. The coset SU(6)/SO(6) contains in addition a color triplet $\mathcal{V}_3^\mu$, a color sextet $\mathcal{A}_6^\mu$ and a color sextet pNGB π_6 whereas the SU(6)/Sp(6) contains in addition a color sextet $\mathcal{V}_6^\mu$, a color triplet $\mathcal{A}_3^\mu$ and a color triplet pNGB π_3. The electric charges of the triplet and sextet states depend on the model details and are summarized in table 1.

In ref. [26, 46], to which we refer for details, the hidden symmetry approach [47] has been used to obtain the effective Lagrangian for these states. In the following we denote the mass of the octet vector by $M_{\mathcal{V}_8}$, the mixing angle between these states and the gluons by β_8 and gauge coupling of the new strong sector by $\tilde{g}$. The main decay modes of the heavy spin-1 resonances are generated by three types of interactions:

- couplings to pNGBs from the chiral Lagrangian in the strong sector;
- couplings to quarks via the mixing of the colour octet to gluons;
- partial compositeness couplings to top and bottom quarks.

The first type stems directly from the pNGB embedding in the effective Lagrangian. It turns out that only two operators contribute [26, 46]

$$O_{\mathcal{V}} = \mathrm{i}\,\mathrm{tr}([\boldsymbol{\pi}, \partial_\mu \boldsymbol{\pi}]\boldsymbol{V}^\mu), \tag{1}$$

$$O_{\mathcal{A}} = \mathrm{tr}([\boldsymbol{\pi}, [\boldsymbol{\pi}, \partial_\mu \boldsymbol{\pi}]]\,\boldsymbol{\mathcal{A}}^\mu)\,, \tag{2}$$

if one requires to have at most three pNBGs at a vertex. Both, O_V and $O_{\mathcal{A}}$ are hermitian. The corresponding coupling of the octet vector is given by

$$C_{\mathcal{V}_8} = \frac{g_{\rho\pi\pi}}{\cos\beta_8} + 2\frac{1+R^2}{1-R^2} g_s \tan\beta_8\,, \tag{3}$$

[1] This is actually an abuse of language. Only in case of the coset SU(3)×SU(3)/SU(3) the names 'vector' and 'axial-vector´ coincides with the CP properties of the spin-1 resonances.

where $g_{\rho\pi\pi}$ is the coupling of the pNGBs to the vector states before any mixing is taken into account and R is a parameter combination of order one [26, 46]. The second type of couplings originates from the mixing of the gluon with $\mathcal{V}_8$, hence yielding a universal couplings of the massive resonance to quarks:

$$\mathcal{L}_{\text{fermions}} = -g_s \tan\beta_8 \, \bar{q} \, \mathcal{V}_8^a t_{\mathbf{3}}^a \, q \equiv C_{\mathcal{V}_8}^{qq} O_{\mathcal{V}_8}^{qq} \,, \tag{4}$$

The third type is generated by the coupling of the spin-1 resonances to the baryons [48, 49] that mix to top and bottom quarks via the partial compositeness mechanism. Although the couplings generated by the strong dynamics are inherently vector-like, the chiral mixing of the physical states generates chiral couplings to the mass eigenstates leading to

$$\mathcal{L}_{\text{PC}} = \bar{t} \mathcal{V}_8^a t_{\mathbf{3}}^a \left(g_{\rho tt,LL} P_L + g_{\rho tt,RR} P_R \right) t + \bar{b} \mathcal{V}_8^a t_{\mathbf{3}}^a \left(g_{\rho bb,LL} P_L \right) b \,. \tag{5}$$

Note that these couplings are of order $\tilde{g}$, while the chiralities are distinguished by the different mixing angles from partial compositeness. Last but not least, note that, while the first two types of couplings are completely determined by the chiral Lagrangian, the third one is more model dependent. The value of the couplings depend on the quantum numbers of baryons that mix with the elementary top and bottom fields, and on the value of the mixing angles. Hence, they cannot be predicted in a model-independent way and we will leave them as free parameters. The relevant parameters of the chiral Lagrangian can be chosen as

$$\tilde{g}, \quad g_{\rho\pi\pi}, \quad M_{\mathcal{V}_8}, \quad \xi = \frac{M_{\mathcal{A}}}{M_{\mathcal{V}_8}} \quad \text{and} \quad f_\chi \,, \tag{6}$$

with f_χ being the decay constant of the color charged pNGBs. $M_{\mathcal{A}}$ is the mass of the axial-vectors.

3. Results

We will assume in the following a lattice and QCD inspired mass hierarchy, where the color charged top-partners are heavier than the spin-1 states, which are heavier than the pNGBs. As mentioned above, the quantum numbers of the lightest coloured resonances are given in terms of the underlying hyperfermions for the twelve models considered. They are listed in table 1 and can be group into five classes. We focus in the following on the color octet $\mathcal{V}_8$, which can be singly produced at the LHC, and present limits due to existing LHC data. For this purpose we have first to recall the properties of the coloured pNGBs, which appear as intermediate decay products. Their phenomenology has been studied in detail in refs. [10, 16, 17] and we summarize here only their main features.

The ubiquitous colour octet pNGB has two types of couplings: a coupling to gauge bosons generated by a topological anomaly and one to top quarks[2] generated by partial compositeness [10, 17]. Their origin is rather different in nature and, thus, their relative importance is rather model dependent. The decays of the other colored charged pNGBs depend crucially on the scenario.

[2]The corresponding one to bottom quarks is suppressed by the ratio m_b/m_t and, thus, is neglected here.

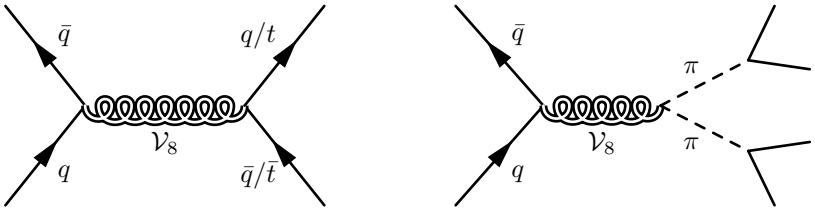

Figure 1: Feynman diagrams of $\mathcal{V}_8$ single production and decay into quarks or pNGBs.

Following the classification in Table 1, we distinguish four cases:

$$\text{C1}: \quad \pi_8 \to t\bar{t},\, gg;\ \pi_6 \to bb\,, \tag{7}$$

$$\text{C2}: \quad \pi_8 \to t\bar{t},\, gg;\ \pi_6 \to tt\,, \tag{8}$$

$$\text{C3}: \quad \pi_8 \to t\bar{t},\, gg;\ \pi_3 \to \bar{b}\bar{s} \text{ or } t\bar{\nu},\, b\tau^+\,, \tag{9}$$

$$\text{C4-5}: \quad \pi_8 \to t\bar{t},\, gg\,. \tag{10}$$

In scenario C2, the sextet has baryon number $2/3$ and electric charge $4/3$. Therefore, partial compositeness leads to an unsuppressed coupling to two right-handed top quarks [16]. In case of scenarios C1 and C3, the sextet and triplet have baryon number $\mp 1/3$ and charges $\mp 2/3$, respectively. Consequently, they are in general not allowed to decay into standard model fermions by partial compositeness alone[3]. Their decays must, therefore, be generated by specific operators that need to violate either baryon number or lepton number leading to the decay channels listed above. The di-quark final states bb and $\bar{b}\bar{s}$ violate baryon number by one unit, $\Delta B = 1$. For π_3 decays to a quark and a lepton[4] can be envisioned, violating lepton number by one unit, $\Delta L = 1$, which can be generated in some models extending partial compositeness to leptons [23]. Note, that while the B or L violating couplings can be rather small, they provide the only decay channel for the corresponding pNGB. We assume here that these couplings are sufficiently large to allow for prompt decays.

The colour octet π_8 can be searched at the LHC via QCD pair production. We assume here that the top couplings dominate leading to a four tops final state. A recent reinterpretation [56] of a CMS search [57] leads to a conservative lower bound of 1.25 TeV for its mass. We note for completeness, that in C2 models, the contribution of π_6 can push this limit further up. Dedicated searches also exist for the leptoquark decays of the triplet in C3 models, where both $b\tau$ and $t\nu$ final states have been searched for by ATLAS and CMS [58–62] yielding bounds in the range 1.25 – 1.46 TeV, depending on the relative size of the branching ratios. The bounds on this mass are significantly lower of about 770 GeV if π_3 decays dominantly into light quarks [63, 64].

In the following we consider single production of $\mathcal{V}_8$ with subsequent decays either into two quarks or into two pNGBs as shown in fig. 1. The possible decay modes of $\mathcal{V}_8$ can be classified as

[3] However, for model M5 there are conceivable scenarios [23] in which the lightest color neutral spin-1/2 resonance $\tilde{b}$ could be lighter than π_3. This would lead to signatures like in supersymmetric models as $\tilde{b}$ is stable. Here π_3 has similar properties as a scalar top quark which decays either in $\tilde{b}t$ or $\tilde{b}W^+\bar{b}$ [50–52]. However, such scenarios requires an extra study beyond the scope of this contribution.

[4] Effectively this is a third generation leptoquark like the ones discussed in [53, 54] or R-partiy violating decays of a scalar top quark in supersymmetric models [55].

follows:

$$\text{C1-2}: \quad \mathcal{V}_8 \to q\bar{q},\ b\bar{b},\ t\bar{t},\ \pi_8\pi_8,\ \pi_6\pi_6^c, \tag{11}$$

$$\text{C3}: \quad \mathcal{V}_8 \to q\bar{q},\ b\bar{b},\ t\bar{t},\ \pi_8\pi_8,\ \pi_3\pi_3^c, \tag{12}$$

$$\text{C4-5}: \quad \mathcal{V}_8 \to q\bar{q},\ b\bar{b},\ t\bar{t},\ \pi_8\pi_8\,. \tag{13}$$

Scenarios C1 and C2 are distinguished by the decays of π_6. The decays into light quarks $q = u, d, c, s$ feature flavour-independent branching ratios, while bottom and top quark channels receive additional contributions from partial compositeness, see eq. (5), leading to different branching ratios. Finally, the relative strength of the pNGB channels is determined purely by colour factors

$$\frac{\text{BR}(\pi_6\pi_6^c)}{\text{BR}(\pi_8\pi_8)} = \frac{10}{3}\,, \qquad \frac{\text{BR}(\pi_3\pi_3^c)}{\text{BR}(\pi_8\pi_8)} = \frac{2}{3}\,. \tag{14}$$

Here we have assumed that their masses are equal.

The importance of each channel depends on the parameter space as can be seen in fig. 2 which provides some benchmarks for the three cosets as illustration. The various features can be understood as follows: the partial width into light quarks is controlled by the mixing angle β_8 to gluons which decreases for increasing $\tilde{g}$. The partial width to pNGBs receives a dominant contribution proportional to $g_{\rho\pi\pi}$. Here the dependence on $\tilde{g}$ is such that this partial width also decreases for increasing $\tilde{g}$. For very small $\tilde{g}$, instead, the second term in eq. (3) starts becoming relevant. This explains the drop in the qq branching ratio observed in fig. 2. Moreover, the scaling in $\tilde{g}$ also explains why the total width of $\mathcal{V}_8$ increases for small values of $\tilde{g}$. We have indicated the regions where the total width becomes large by different grey shadings. Finally, the branching ratio to top (and bottom) receives a dominant contribution from partial compositeness by our choice of parameters. Thus, they dominate for large values as they do not scale with $\tilde{g}$.

The couplings of $\mathcal{V}_8$ to the light quarks allows for single production, see fig. 1. The current bounds on the colour octet mass crucially depend on the branching ratios in the above discussed three channels: light quarks, pNGBs and top quarks. They are controlled by different couplings. As a model-independent estimate of the bounds we, therefore, decided to show limits assuming 100% branching ratios in the three channels, as shown in fig. 3 for the scenarios C1, C2 and C3. The bounds in scenario C4-5 are very similar to the ones of scenario C2, see refs. [26, 46] to which we refer for further details. The bounds are extracted from the following searches:

- di-jet: search for high mass di-quark resonances [65];
- di-top: search for $t\bar{t}$ resonances [66];
- pNGBs: recasts of SUSY searches [67–69] implemented in `CheckMATE` [70, 71].

The colours indicate the Drell-Yan type cross section, which depends only on $\tilde{g}$ and $M_{\mathcal{V}_8}$. The region below and to the left of the lines is excluded. The results show that the limits on the mass are roughly the same in the range of 4 to 5 TeV for all scenarios. Note however, that the region for small $\tilde{g} \lesssim 3$ cannot be fully trusted as it corresponds to widths above 50% of the mass and, thus, a dedicated analysis would be required which however is beyond the scope of this contribution.

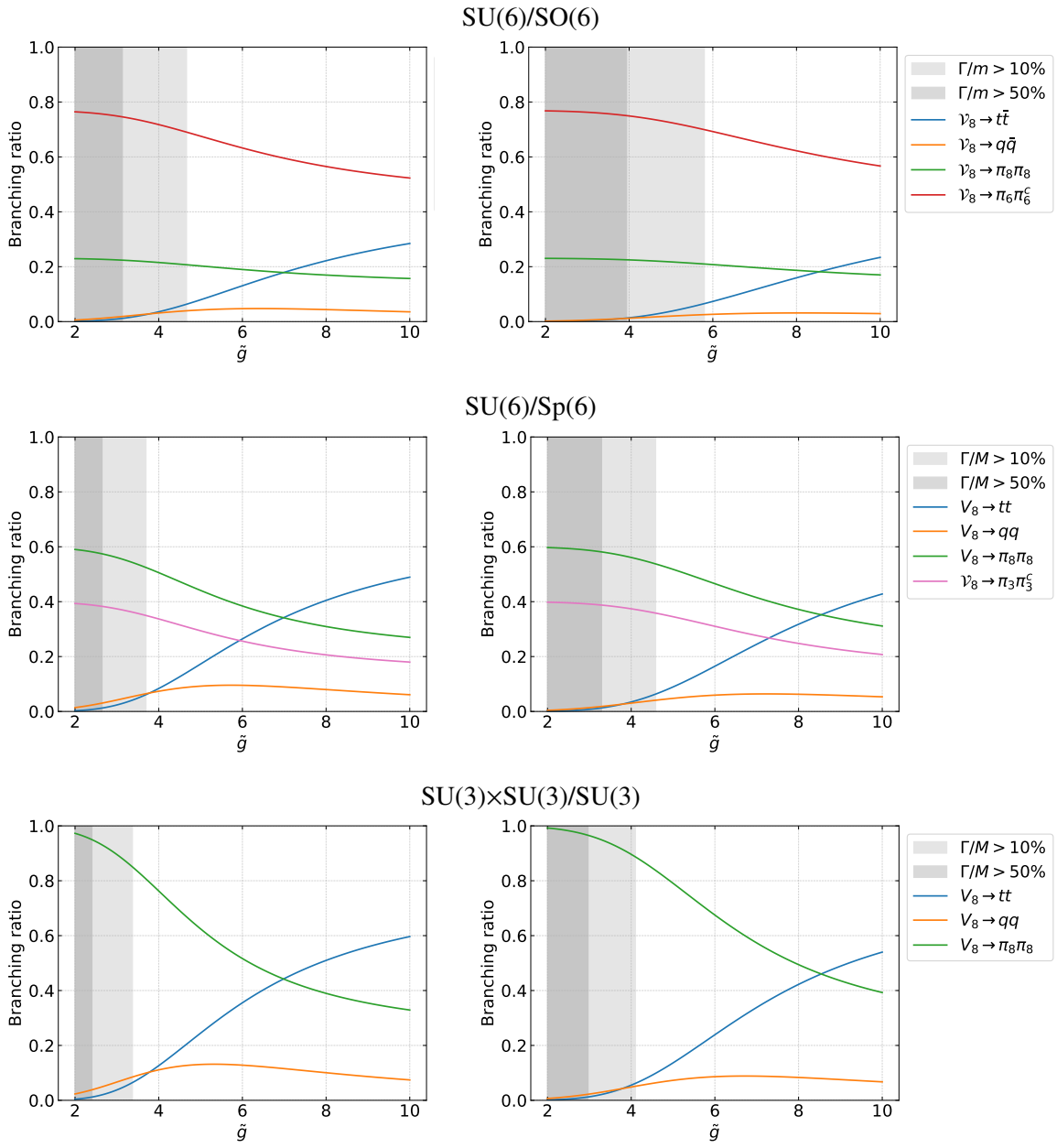

Figure 2: $\mathcal{V}_8$ branching ratios for the various cosets as a function of $\tilde{g}$ for $M_{\mathcal{V}_8} = 4.5$ TeV, $g_{\rho\pi\pi} = 1$, $m_\pi = 1.4$ TeV, $f_\chi = 1$ TeV and fixing the coupling to top quarks to 1. We have fixed in the left column $\xi = 1$ and in the right column $\xi = 1.4$. Moreover, $q = u, d, s, c, b$.

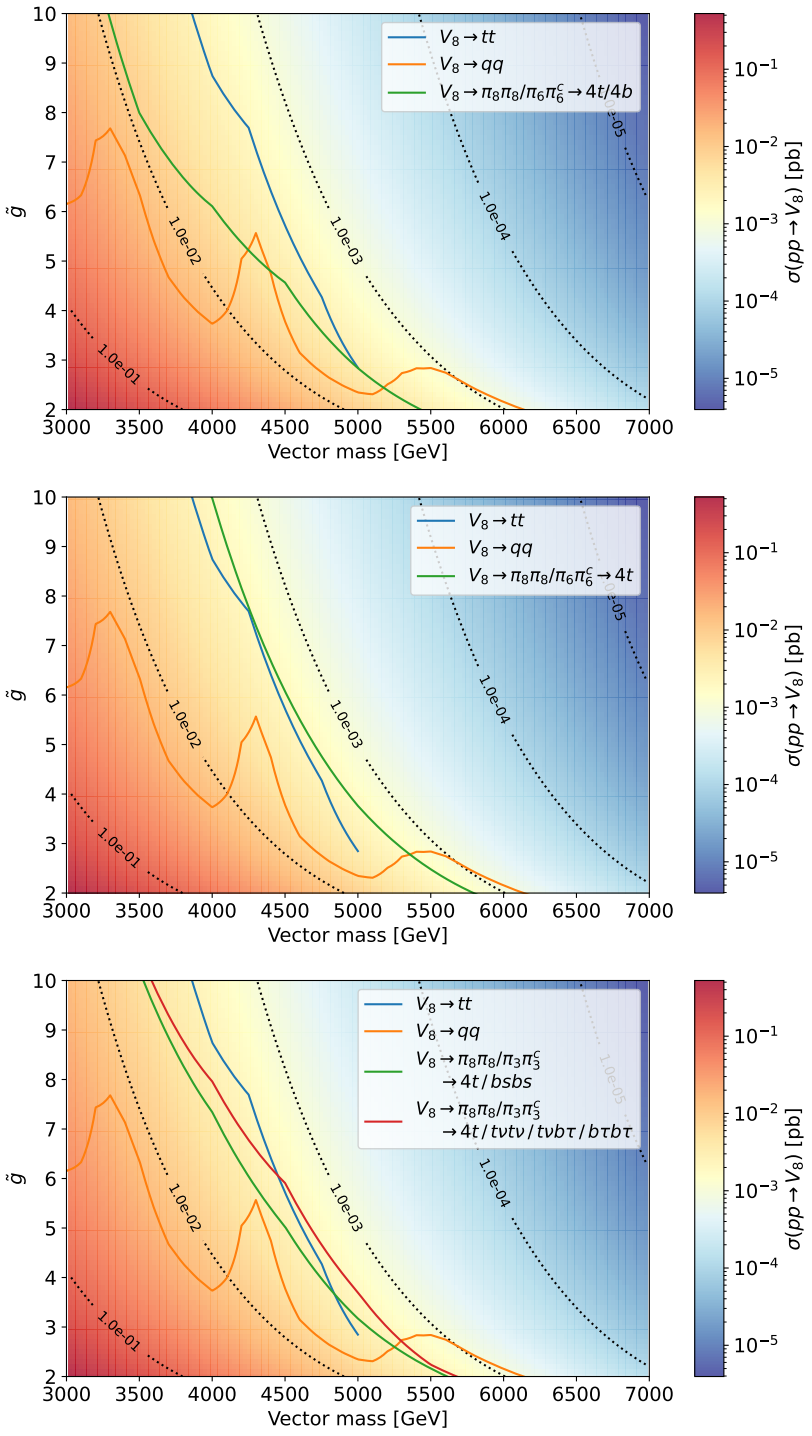

Figure 3: Bounds on vector octet single production for the model classes C1 (top), C2 (middle) and C3 (bottom) defined in table 1. The colors and the dotted contours indicate the single production cross section. The region to the left and below the coloured lines is excluded. The bounds are determined assuming 100% branching ratio into the indicated channel. For the decays into pNGBs, the ratios of branching ratios in eq. (14) are taken into account.

4. Discussion and outlook

We have presented the LHC phenomenology of spin-1 resonances carrying QCD charges in Composite Higgs Models with a focus on models which allow for fermionic UV completions [9, 10]. More precisely, we have worked out their properties for three types of cosets, SU(6)/SO(6), SU(6)/Sp(6) and SU(3)×SU(3)/SU(3) including their most relevant production at the LHC and their decay channels. These are symmetric cosets and, thus, they contain two sets of spin-1 resonances: vector states that coupling to two or more pNGBs and axial-vector states which have to couple to at least three pNGBs.

All scenarios feature a vector $\mathcal{V}_8$ which mixes with the gluons. As a consequence, $\mathcal{V}_8$ can be singly produced at hadron colliders via Drell-Yan, whereas all other states can only be pair-produced. The $\mathcal{V}_8$ can either decay into a quark pair or into two pNGBs leading in all cases to the final states $q\bar{q}$ ($q \neq t$), $t\bar{t}$ and $4t$. We have investigated the bounds on $\mathcal{V}_8$ from current LHC data. For this we have used on the one hand direct searches for resonances decaying to two SM quarks. In the other hand, we have used recasts from searches for supersymmetric particles for cascade decays via pNGBs. We have found in all scenarios bounds on its mass ranging from 3.5 TeV to 6 TeV. However, we note for completeness that in some part of parameter space these results has to be taken with a grain of salt as this resonance has a rather broad total decay width which calls for a detailed reanalysis of the data.

The high luminosity run at the LHC will certainly allow to further improve the mass limits on $\mathcal{V}_8$. However, already the current bounds in Fig. 3 imply that pair production of all spin-1 resonances will have rather small cross sections at the LHC, hence making their detection unlikely. Thus, we briefly sketch here their signatures from pair production at a future high energy hadron collider, e.g. a prospective 100 TeV pp collider, which will be presented more detail in a future contribution. However, we should stress that single production of $\mathcal{V}_8$ remains the leading discovery channel and, thus, one would expect to discover $\mathcal{V}_8$ before pair production becomes relevant.

The sextets, which feature the largest pair production cross sections [26], are present in scenarios C1, C2 and C3. Their decays can be classified as follows:

$$\mathcal{A}_6 \;\to\; \pi_8\pi_8\pi_6\;(t\bar{t}t\bar{t}bb) \;\text{ and }\; \pi_6\pi_6^c\pi_6\;(\bar{b}\bar{b}bbbb) \quad \text{in C1}\,, \tag{15}$$

$$\mathcal{A}_6 \;\to\; tt \text{ or } \pi_8\pi_8\pi_6\;(t\bar{t}t\bar{t}tt) \;\text{ and }\; \pi_6\pi_6^c\pi_6\;(\bar{t}\bar{t}tttt) \quad \text{in C2}\,, \tag{16}$$

$$\mathcal{V}_6 \;\to\; \pi_8\pi_3^c \to (t\bar{t})(\bar{b}\bar{s} \text{ or } ql) \quad \text{in C3}\,. \tag{17}$$

The two-body decay of $\mathcal{V}_6$ in C3 is driven by $g_{\rho\pi\pi}$, hence is will likely imply a large decay width. By contrast, thanks to the three body final state of $\mathcal{A}_6$ in pNGBs, one expects the widths of $\mathcal{A}_6$ to remain small compared to its mass. In scenarios C2, $\mathcal{A}_6$ can also decay into two tops which however is suppressed by $v^2/f^2 \leq 0.04$ (for $f \geq 1$ TeV). At the same time the three-pNGB channel is suppressed by a phase space factor and, thus, one expects that both decay modes will compete and that the widths remain small for these states. In both cases, C1 and C2, the pair production of $\mathcal{A}_6$ will lead to final states containing several top and bottom jets.

The axial colour octet $\mathcal{A}_8$ also has a sizeable pair cross section but somewhat smaller than the ones of the sextets. Its leading decay channel is into two tops in all cases. Thus, one has a four-top final state with potentially large width effects.

Scenarios C1, C2 and C3 features in addition the colour triplets which have cross sections which are roughly an order of magnitude smaller if all spin-1 resonances have about the same mass. They have the following decays:

$$\mathcal{V}_3 \to \pi_8\pi_6^c \ (t\bar{t}\bar{b}\bar{b}) \quad \text{in C1}\,, \tag{18}$$

$$\mathcal{V}_3 \to \bar{t}\bar{t} \text{ or } \pi_8\pi_6^c \ (t\bar{t}\bar{t}\bar{t}) \quad \text{in C2}\,, \tag{19}$$

$$\mathcal{A}_3 \to \pi_8\pi_8\pi_3 \ (t\bar{t}t\bar{t} + \bar{b}\bar{s} \text{ or } ql) \text{ or } \pi_3\pi_3^c\pi_3 \ (\bar{b}\bar{s}bs\bar{b}\bar{s} \text{ or } ql\bar{q}lql) \quad \text{in C3}\,. \tag{20}$$

$\mathcal{V}_3$ will mainly decay into $\pi_8\pi_6^c$ independent of the scenario as the di-top coupling in C2 is suppressed by v/f. One expects a large total decay width in most of the allowed parameter space. In contrast, the $\mathcal{A}_3$ in C3 will be a narrow resonance with interesting final states rich in top quarks and possibly leptons, if the π_3 decays violate lepton number.

Acknowledgments

I thank G. Cacciapaglia, A.S. Cornell, A. Deandrea, T. Flacke, M. Kunkel and R. Ströhmer for interesting and fruitful discussions. I thank M. Kunkel for creating the plots in fig. 2. I also would like to thank the organizers of the Corfu workshops for creating such a stimulating environment. This work has been supported by DFG project nr PO/1337-12/1.

References

[1] D. B. Kaplan and H. Georgi, Phys. Lett. B **136** (1984), 183-186

[2] D. B. Kaplan, H. Georgi and S. Dimopoulos, Phys. Lett. B **136** (1984), 187-190

[3] R. Contino, Y. Nomura and A. Pomarol, Nucl. Phys. B **671** (2003), 148-174 [arXiv:hep-ph/0306259 [hep-ph]].

[4] K. Agashe, R. Contino and A. Pomarol, Nucl. Phys. B **719** (2005), 165-187 [arXiv:hep-ph/0412089 [hep-ph]].

[5] J. Galloway *et al.*,JHEP **10** (2010), 086 [arXiv:1001.1361 [hep-ph]].

[6] G. Cacciapaglia and F. Sannino, JHEP **04** (2014), 111 [arXiv:1402.0233 [hep-ph]].

[7] D. B. Kaplan, Nucl. Phys. B **365** (1991), 259-278

[8] G. Ferretti and D. Karateev, JHEP **03** (2014), 077 [arXiv:1312.5330 [hep-ph]].

[9] G. Ferretti, JHEP **06** (2016), 107 [arXiv:1604.06467 [hep-ph]].

[10] A. Belyaev *et al.*,JHEP **01** (2017), 094 [erratum: JHEP **12** (2017), 088] [arXiv:1610.06591 [hep-ph]].

[11] A. Agugliaro *et al.*,JHEP **02** (2019), 089 [arXiv:1808.10175 [hep-ph]].

[12] G. Cacciapaglia *et al.*,JHEP **12** (2022), 087 [arXiv:2210.01826 [hep-ph]].

[13] T. Flacke *et al.*,JHEP **11** (2023), 009 [arXiv:2304.09195 [hep-ph]].

[14] G. Cacciapaglia *et al.*,Front. in Phys. **7** (2019), 22 [arXiv:1902.06890 [hep-ph]].

[15] D. Buarque Franzosi *et al.*,Eur. Phys. J. C **82** (2022) no.1, 3 [arXiv:2106.12615 [hep-ph]].

[16] G. Cacciapaglia *et al.*,JHEP **11** (2015), 201 [arXiv:1507.02283 [hep-ph]].

[17] G. Cacciapaglia *et al.*,JHEP **05** (2020), 027 [arXiv:2002.01474 [hep-ph]].

[18] N. Bizot, G. Cacciapaglia and T. Flacke, JHEP **06** (2018), 065 [arXiv:1803.00021 [hep-ph]].

[19] K. P. Xie, G. Cacciapaglia and T. Flacke, JHEP **10** (2019), 134 [arXiv:1907.05894 [hep-ph]].

[20] G. Cacciapaglia *et al.*,Phys. Lett. B **798** (2019), 135015 [arXiv:1908.07524 [hep-ph]].

[21] A. Banerjee, D. B. Franzosi and G. Ferretti, JHEP **03** (2022), 200 [arXiv:2202.00037 [hep-ph]].

[22] A. Banerjee *et al.*,SciPost Phys. Core **7** (2024), 079 [arXiv:2406.09193 [hep-ph]].

[23] G. Cacciapaglia *et al.*,JHEP **02** (2022), 208 [arXiv:2112.00019 [hep-ph]].

[24] D. Buarque Franzosi *et al.*,JHEP **11** (2016), 076 [arXiv:1605.01363 [hep-ph]].

[25] R. Caliri *et al.*,[arXiv:2412.08720 [hep-ph]].

[26] G. Cacciapaglia *et al.*,JHEP **06** (2024), 092 [arXiv:2404.02198 [hep-ph]].

[27] E. Bennett *et al.*,JHEP **03** (2018), 185 [arXiv:1712.04220 [hep-lat]].

[28] E. Bennett *et al.*,Phys. Rev. D **101** (2020) no.7, 074516 [arXiv:1912.06505 [hep-lat]].

[29] E. Bennett *et al.*,JHEP **12** (2019), 053 [arXiv:1909.12662 [hep-lat]].

[30] E. Bennett *et al.*,Phys. Rev. D **106** (2022) no.1, 014501 [arXiv:2202.05516 [hep-lat]].

[31] S. Kulkarni *et al.*,SciPost Phys. **14** (2023) no.3, 044 [arXiv:2202.05191 [hep-ph]].

[32] E. Bennett *et al.*,Phys. Rev. D **109** (2024) no.9, 094512 [arXiv:2311.14663 [hep-lat]].

[33] E. Bennett *et al.*,[arXiv:2412.01170 [hep-lat]].

[34] V. Ayyar *et al.*,Phys. Rev. D **97** (2018) no.7, 074505 [arXiv:1710.00806 [hep-lat]].

[35] V. Ayyar *et al.*,Phys. Rev. D **99** (2019) no.9, 094502 [arXiv:1812.02727 [hep-ph]].

[36] V. Ayyar *et al.*,Phys. Rev. D **97** (2018) no.11, 114502 [arXiv:1802.09644 [hep-lat]].

[37] V. Ayyar *et al.*,Phys. Rev. D **97** (2018) no.11, 114505 [arXiv:1801.05809 [hep-ph]].

[38] V. Ayyar *et al.*,Phys. Rev. D **99** (2019) no.9, 094504 [arXiv:1903.02535 [hep-lat]].

[39] A. Hasenfratz *et al.*,Phys. Rev. D **107** (2023) no.11, 114504 [arXiv:2304.11729 [hep-lat]].

[40] J. Erdmenger *et al.*,Phys. Rev. Lett. **126** (2021) no.7, 071602 [arXiv:2009.10737 [hep-ph]].

[41] J. Erdmenger *et al.*,JHEP **02** (2021), 058 [arXiv:2010.10279 [hep-ph]].

[42] D. Elander *et al.*,JHEP **03** (2021), 182 [arXiv:2011.03003 [hep-ph]].

[43] D. Elander *et al.*,JHEP **05** (2022), 066 [arXiv:2112.14740 [hep-ph]].

[44] J. Erdmenger *et al.*,Universe **9** (2023) no.6, 289 [arXiv:2304.09190 [hep-th]].

[45] J. Erdmenger *et al.*,JHEP **07** (2024), 169 [arXiv:2404.14480 [hep-ph]].

[46] M. Kunkel, 'Collider Phenomenology of Composite Higgs Models', PhD-thesis, Würzburg 2024, doi:10.25972/OPUS-39149

[47] M. Bando, T. Kugo and K. Yamawaki, Phys. Rept. **164** (1988), 217-314

[48] G. Erkol, R. G. E. Timmermans and T. A. Rijken, Phys. Rev. C **74** (2006), 045201

[49] T. M. Aliev *et al.*,Phys. Rev. D **80** (2009), 016010 [arXiv:0905.4664 [hep-ph]].

[50] W. Porod and T. Wöhrmann, Phys. Rev. D **55** (1997), 2907-2917 [erratum: Phys. Rev. D **67** (2003), 059902] [arXiv:hep-ph/9608472 [hep-ph]].

[51] W. Porod, Phys. Rev. D **59** (1999), 095009 [arXiv:hep-ph/9812230 [hep-ph]].

[52] C. Boehm, A. Djouadi and Y. Mambrini, Phys. Rev. D **61** (2000), 095006 [arXiv:hep-ph/9907428 [hep-ph]].

[53] T. Faber *et al.*,Phys. Lett. B **787** (2018), 159-166 [arXiv:1808.05511 [hep-ph]].

[54] T. Faber *et al.*, Phys. Rev. D **101** (2020) no.9, 095024 [arXiv:1812.07592 [hep-ph]].

[55] D. Restrepo, W. Porod and J. W. F. Valle, Phys. Rev. D **64** (2001), 055011 [arXiv:hep-ph/0104040 [hep-ph]].

[56] L. Darmé, B. Fuks and F. Maltoni, JHEP **09** (2021), 143 [arXiv:2104.09512 [hep-ph]].

[57] A. M. Sirunyan *et al.* [CMS], Eur. Phys. J. C **80** (2020) no.2, 75 [arXiv:1908.06463 [hep-ex]].

[58] G. Aad *et al.* [ATLAS], Phys. Rev. D **104** (2021) no.11, 112005 [arXiv:2108.07665 [hep-ex]].

[59] A. M. Sirunyan *et al.* [CMS], Phys. Lett. B **819** (2021), 136446 [arXiv:2012.04178 [hep-ex]].

[60] A. Hayrapetyan *et al.* [CMS], JHEP **05** (2024), 311 [arXiv:2308.07826 [hep-ex]].

[61] G. Aad *et al.* [ATLAS], Eur. Phys. J. C **83** (2023) no.11, 1075 [arXiv:2303.01294 [hep-ex]].

[62] G. Aad *et al.* [ATLAS], Phys. Lett. B **854** (2024), 138736 [arXiv:2401.11928 [hep-ex]].

[63] M. Aaboud *et al.* [ATLAS], Eur. Phys. J. C **78** (2018) no.3, 250 [arXiv:1710.07171 [hep-ex]].

[64] A. Tumasyan *et al.* [CMS], JHEP **07** (2023), 161 [arXiv:2206.09997 [hep-ex]].

[65] A. M. Sirunyan *et al.* [CMS], JHEP **05** (2020), 033 [arXiv:1911.03947 [hep-ex]].

[66] G. Aad *et al.* [ATLAS], JHEP **10** (2020), 061 [arXiv:2005.05138 [hep-ex]].

[67] G. Aad *et al.* [ATLAS], JHEP **06** (2020), 046 [arXiv:1909.08457 [hep-ex]].

[68] G. Aad *et al.* [ATLAS], Eur. Phys. J. C **81** (2021) no.7, 600 [erratum: Eur. Phys. J. C **81** (2021) no.10, 956] [arXiv:2101.01629 [hep-ex]].

[69] G. Aad *et al.* [ATLAS], Eur. Phys. J. C **83** (2023) no.7, 561 [arXiv:2211.08028 [hep-ex]].

[70] M. Drees *et al.*,Comput. Phys. Commun. **187** (2015), 227-265 [arXiv:1312.2591 [hep-ph]].

[71] D. Dercks *et al.*,Comput. Phys. Commun. **221** (2017), 383-418 [arXiv:1611.09856 [hep-ph]].